NRL Report 8104

Atmospheric Transmission Measurement Program Report for 1 July Through 30 September 1976 (TQ 1976)

T. H. COSDEN, J. A. CURCIO, J. A. DOWLING, C. O. GOTT, D. H. GARCIA, S. T. HANLEY, K. M. HAUGHT, R. F. HORTON, AND G. L. TRUSTY

Optical Radiation Branch
Optical Sciences Division

and

W. L. AGAMBAR

Potomac Research Inc.
McLean, Virginia

September 1, 1977

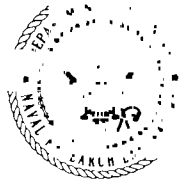

NAVAL RESEARCH LABORATORY
Washington, D.C.

REPORT DOCUMENTATION PAGE

READ INSTRUCTIONS BEFORE COMPLETING FORM

1. REPORT NUMBER: NRL Report 8104
2. GOVT ACCESSION NO.:
3. RECIPIENT'S CATALOG NUMBER:

4. TITLE (and Subtitle): ATMOSPHERIC TRANSMISSION MEASUREMENT PROGRAM REPORT FOR 1 JULY THROUGH 30 SEPTEMBER 1976 (TQ 1976)

5. TYPE OF REPORT & PERIOD COVERED: Interim report on a continuing NRL Problem

6. PERFORMING ORG. REPORT NUMBER:

7. AUTHOR(s): T.H. Cosden, J.A. Curcio, J.A. Dowling, C.O. Gott, D.H. Garcia, S.T. Hanley, K.M. Haught, R.F. Horton, G.L. Trusty, and W.L. Agambar

8. CONTRACT OR GRANT NUMBER(s): NRL Problem R05-31
Project 405-003-173-1-SRSL-40AA76

9. PERFORMING ORGANIZATION NAME AND ADDRESS: Naval Research Laboratory
Washington, D. C. 20375

10. PROGRAM ELEMENT, PROJECT, TASK AREA & WORK UNIT NUMBERS:

11. CONTROLLING OFFICE NAME AND ADDRESS: Department of the Navy
Naval Sea Systems Command (PM-22/PMS-405)
Washington, D.C. 20362

12. REPORT DATE: September 1, 1977

13. NUMBER OF PAGES: 31

14. MONITORING AGENCY NAME & ADDRESS(if different from Controlling Office):

15. SECURITY CLASS. (of this report): Unclassified

15a. DECLASSIFICATION/DOWNGRADING SCHEDULE: Unclassified

16. DISTRIBUTION STATEMENT (of this Report)

Approved for public release; distribution unlimited

17. DISTRIBUTION STATEMENT (of the abstract entered in Block 20, if different from Report)

18. SUPPLEMENTARY NOTES

19. KEY WORDS (Continue on reverse side if necessary and identify by block number)

Lasers
Atmospheric transmission
Fourier spectroscopy
Gas filter correlation spectroscopy

20. ABSTRACT (Continue on reverse side if necessary and identify by block number)

A facility has been completed to measure atmospheric transmission by combining measurement techniques based on laser-line extinction, high-resolution Fourier spectroscopy, and gas filter correlation spectroscopy. Essential features of this measurement system are described, and initial measurements are presented of 0.1-cm^{-1}-resolution atmospheric transmission using a 5-km overwater path at the Patuxent River Naval Air Station, Patuxent River, Maryland. Concurrent absolute transmission

(Continued)

20. Continued

measurements at several DF laser wavelengths between 3.6 and 4.1 μm have been used to provide absolute transmission calibrations for the spectra.

CONTENTS

ATMOSPHERIC TRANSMISSION MEASUREMENTS PROGRAM REPORT FOR 1 JULY THROUGH 30 SEPTEMBER 1976 (TQ 1976)

INTRODUCTION

This report describes the accomplishments of the NRL atmospheric transmission measurement program realized during TQ 1976. During this period the improved facilities for atmospheric transmission studies carried out under the auspices of the Navy HEL/SLTDP (High Energy Laser/Special Laser Technology Development Program) were completed.

Included in this improved facility are a high-resolution infrared interferometer-spectrometer system (a scanning Michelson interferometer (SMI) which includes a self-contained data-processing system) and a gas filter correlation spectrometer (GFCS), each sharing a large-aperture (1.2-m-diameter) receiver optical system.

The SMI and GFCS instruments, the apparatus to measure laser-line extinction, and the receiver optical system are contained in a large van trailer which was suitably modified for use with this instrumentation. This trailer is based on a previously existing unit housing a 1.2-m-diameter f/5 parabolic mirror and mount which was obtained from the Army Ballistic Research Laboratory (BRL) as surplus to their current requirements. The trailer structure was modified, a secondary optical system and mounts were designed, constructed, and installed, and mountings for and installation of the SMI and GFCS instruments were carried out at the Chesapeake Bay Division of NRL (CBD) beginning in March 1976.

Field checkout of this trailer along with the other elements of the Infrared Mobile Optical Radiation Laboratory (IMORL) was begun at CBD once the SMI was installed, approximately 15 July 1976. The entire IMORL facility was moved to the Patuxent River Naval Air Station (NAS), Patuxent River, Maryland, for long-path measurements and equipment shakedown starting 7 September 1976. The long path is the path from A to B in Fig. 1.

Successful operation of the facility has been demonstrated by the measurements documented in this report. Long-path laser transmission measurements at nine DF laser wavelengths have been made in conjunction with high-resolution atmospheric-transmission spectra taken in the DF laser region. The transmission spectra were measured using the same optical systems and atmospheric path used for the laser measurements. In this way the high-resolution spectra are calibrated in terms of absolute transmission. The procedures used in this calibration are described in a later section of this report.

The atmospheric-measurements-program accomplishments documented in this report address the original SLTDP goal:

Manuscript submitted January 10, 1977.

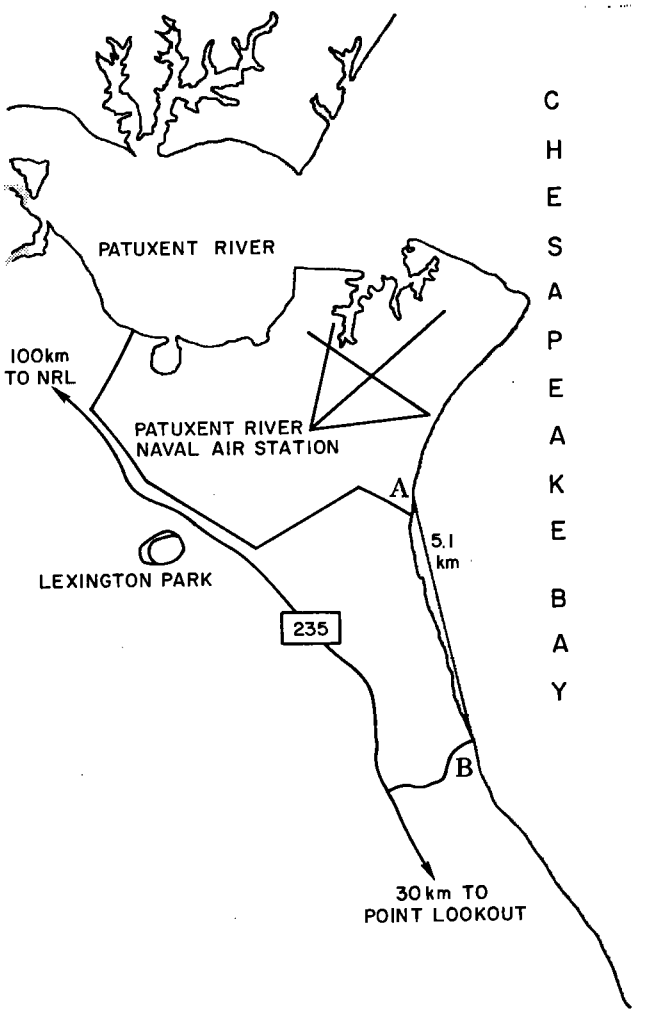

Fig. 1—Experimental Sites

To verify existing atmospheric-transmission predictive capability (HI-TRAN code and AFGL spectral-line-parameter data tape) and to identify inaccuracies of such predictions by means of comparisons to field measurements of infrared transmission using laser sources and Fourier spectroscopy for a wide variety of atmospheric conditions.

The SLTDP-funded activities within the NRL atmospheric-measurement program have included the implementation of a small CW DF laser and extinction-measurement apparatus suitable for field measurements and the subsequent use of these equipments in several field experiments. These experiments have yielded an extensive data base used to compare measured DF-laser-line extinction to predictions.

Joint SLTDP and DARPA funding has been directed toward complementary laboratory measurements and an analysis program carried out by contract with Science Applications, Inc., Ann Arbor, Michigan. This work has provided measurements and model comparisons needed to predict the transmission of DF laser frequencies for a wide variety of atmospheric conditions. These predictions in turn have been verified by comparisons to the data generated by the NRL field measurements.

The incorporation of the SMI and GFCS instruments into the IMORL facility as documented in this report represents the most recent activity funded under the SLTDP. The use of the present augmented facility in carrying out the field measurements required for verification of predictive models for laser-beam transmission is to be accomplished under the Navy HEL baseline technology program. In the sections that follow, this report provides references to earlier field experiments carried out under this program, summarizes the TQ 1976 activities recently completed, briefly describes the facilities now in use, presents the initial proof-of-performance measurements obtained at the Patuxent River NAS, and compares the measurements to synthetic high-resolution spectra calculated for atmospheric conditions closely corresponding to those of the measurements.

BACKGROUND

Field experiments designed to validate atmospheric transmission predictions for several important infrared laser lines have been carried out during the past 3 years by the NRL field-measurement team. Extensive experiments involving the measurement of long-path transmission values at several infrared wavelengths (principally in the 3.6- to 4.1-μm DF laser region) in conjunction with detailed characterization of atmospheric conditions have been conducted at sites in Florida [1,2] and California [3]. Discrepancies between predicted values and the results obtained in such experiments have been addressed by careful laboratory measurements designed to update the absorption-line parameter values used in the calculations [4,5].

Improved predictions of DF-laser-line transmission (as verified by the NRL field experiments) have been supplied to the user community as requested and as such information became available. Several recent and forthcoming reports [2–7] document both the field-measurement instrumentation, the experimental results, and the comparison of field data with transmission predictions.

The near-term objective of the field-measurement program through TQ 1976 was the demonstration of a working capability to perform high-resolution atmospheric-transmission

measurements over a 5.1-km path in the DF spectral region (2500 to 2800 cm^{-1}) using a scanning Michelson interferometer (SMI), 1.2-m-aperture receiver telescope, and absolute transmission calibrations by means of selected DF laser transmission measurements.

This objective has been satisfied by the results, which are presented in later sections of this report. The execution of the field measurements and submission of this report are in conformance with the TQ 1976 test plan recently submitted to the PM 22 program office.

SUMMARY OF ACTIVITIES FOR TQ 1976

Field-Measurement Program

The principal activities early in TQ 1976 were devoted to completing the structure modifications and fabricating and installing the optical system in the optical receiver trailer described in the Introduction. Figure 2 is a diagram of the interior of this trailer in its present configuration showing a plan view of the collector optical system and location of the GFCS and SMI instruments and the SMI data console.

Modifications to the trailer structure included the addition of an enclosure surrounding the incoming optical beam and a 1-meter extension of the trailer to enclose the transfer optical system consisting of the mirrors E1, F1, F2, and the small recollimating parabolic mirror opposite E1. A roll-up door was installed in the newly constructed end of the trailer to provide a 1.2-by-1.5-m opening for the incoming beam. A bench for mounting the GFCS and SMI instruments and intermediate transfer optics was constructed and installed in the trailer as well as a translating optical bench containing the demagnifying and recollimating optics located transversely across the beam input end of the trailer. Each of these benches stands on four legs which extend through the trailer floor and rest on the ground, independent of the trailer structure.

Upon completion of the receiver trailer and delivery of the SMI system from the Carson-Alexiou Corporation, initial checkout of the extinction-measurement apparatus

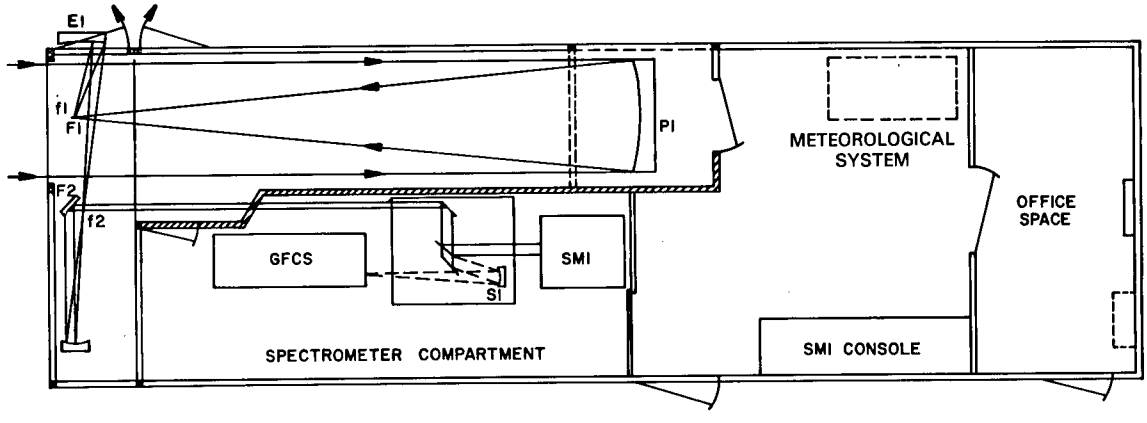

Fig. 2—New receiver-trailer floor plan and optical system

together with the SMI system was begun at CBD, approximately 15 July 1976. "Zero-path" (minimal-path length) calibrations were performed once proper operation of the DF laser system was achieved. The DF laser and F_2 gas supply system had not been in use since the JAN propagation tests performed during June-October 1975 and were subsequently overhauled, with the replacement of the F_2 supply regulator. Between 15 August and 3 September 1976, sufficient tests were performed at CBD using the "zero-path" and the 400-m path which are available there to indicate the experiment could be successfully operated over the 5.1-km path at the Patuxent River NAS.

The several trailers involved in laser transmission, GFCS, and SMI experiments as well as a supply trailer, office trailer housing meteorological instrumentation, and a meteorological van were then relocated to the Patuxent River NAS at site A in Fig. 1. Initial setup was completed, and "zero-path" measurements were performed at that location during 7-18 September 1976. The "zero-path" used at site A is actually a 70-m air path when distances within and between the trailers are included. The receiver trailer and meteorological van were moved to site B on 20 September 1976 to begin long-path measurement. The GFCS instrument was delivered at site A and installed in the receiver trailer prior to its relocation to site B.

Extinction measurements for nine DF laser lines were conducted on 22 and 24 September 1976. High-resolution atmospheric-absorption spectra were recorded over the 5.1-km path between sites A and B on 24 September and were used in an experiment that combined the DF-laser-line transmission measurements with the atmospheric-absorption spectra. These data as well as earlier extinction and meteorological data are presented later in this report.

Supporting Contractual Activities

Contractual support of the NRL field-measurement program carried out during TQ 1976 was provided by Science Applications Inc. (SAI), Ann Arbor, Michigan, and was devoted to the high-resolution laboratory measurement of spectral line profiles and development of absorption algorithms based on these data.

The first SAI task in support of the atmospheric transmission measurement program required high-resolution line-profile measurements of HDO lines important for propagation of DF laser radiation. The 3-m-focal-length Ebert spectrometer used in earlier work [4,5] was used to obtain the data. Techniques developed by SAI for extracting line parameters from blended absorption-line complexes were used. The second task required that continuum absorption important to the DF lines be identified and quantified. Continuum-absorption coefficients are needed to develop complete pressure and temperature scaling algorithms for DF laser propagation and to analyze SMI data.

The contractor's goals originally set forth at the beginning of TQ 1976 for this task have been satisfactorily accomplished. Atmospheric-absorption-line profile data and continuum-absorption coefficients important for the $P_1 11$, $P_1 12$, $P_3 11$, and $P_3 12$ DF laser lines have been obtained, and it has been confirmed that local atmospheric absorption lines are of minor importance for the latter three DF lines: $P_1 12$, $P_3 11$, and $P_3 12$. However for

these three lines continuum absorption by N_2 and H_2O dominates. For both molecules the values of the continuum-absorption coefficients are quite different than those used earlier for three lines.

These new values for the N_2 continuum-absorption coefficient are from Shapiro et al. [8]. These values were adopted and are recommended because the original (Burch) values have been found inaccurate.

The new H_2O continuum values are from the Atmospheric Sciences Laboratory (ASL) at White Sands Missile Range [9]. These values are taken to be most credible, since they were obtained in the laboratory at nearly the pressure and temperature (≈ 300 K) conditions in the real world. The earlier values were obtained by extrapolation from data taken at elevated temperatures and greatly enriched concentrations. The credibility of the ASL (White-cell) data is strengthened in that it agrees with spectrophone data taken independently of the White-cell data. Final resolution of the continuum question may await analysis of NRL long-path SMI data.

The P_1 11 line is dominated by HDO line absorption. Accordingly spectral scans required for extracting line parameters were undertaken and completed. New parameters are listed in Table 1. The bounds on the HDO line absorption coefficients for the

Table 1—Measured HDO-Absorption-Line Strength (S) and Width (γ) Parameters Near the P_1 11 Line

HDO Center Frequency (cm^{-1})	S (per molecule $\times 10^{21}$)	γ (cm^{-1}/atm)
2612.541	11	0.091
2619.762	14	0.098
2622.108	16	0.089
2628.459	15	0.098
2635.600	21	0.094
2637.359	21	0.092
2638.557	23	0.097
2638.728	16	0.091
2644.470	18	0.100
2649.353	28	0.103

remaining DF laser lines are $\lesssim 0.004$ km^{-1} for $P_1 12$, $\lesssim 0.003$ km^{-1} for $P_3 11$, and $\lesssim 0.003$ km^{-1} for $P_3 12$.

Completion of the TQ 1976 program under this task will result in a basic understanding of atmospheric molecular line absorption for DF lasers out to wavelengths of almost 4.1 μm. Beyond 4.1 μm, $v = 4 \rightarrow 3$ DF lines and very high $J\, v = 3 \rightarrow 2$ DF lines occur. These may be important for propagation at the frequencies of the NACL and MIRACL lasers. Also, beyond $\approx$4.6 μm the lowest lying and best propagating CO-laser frequencies occur. In this region between $\approx$5 μm and 4.1 μm, the water continuum is ill defined, and fixed-frequency CO measurements have been in disagreement with HI-TRAN predictions based on the AFCRL data compilation. Consequently the source of CO-laser-frequency propagation uncertainties should be identified, and field-verified algorithms for predicting CO-laser-frequency propagation should be developed. In the process complete modeling of atmospheric molecular absorption may be obtained between 4.1 μm and 4.6 μm, where the highest-lying NACL and MIRACL lines are expected to occur. Recommendations are:

- Perform laboratory high-resolution line-profile scans in the CO-laser region ($\approx$4.6 μm to 5.2 μm);

- Use the laboratory data to extract line parameters important for CO-laser-frequency transmission;

- Confirm scaling laws with NRL field SMI and CO laser data;

- Develop field-verified models for molecular H_2O and N_2 continuum absorption in the spectral gap between the frequencies of the BDL laser and CO lasers;

- Using the above, extract aerosol total-extinction coefficients for eventual development of a total-linear-extinction modeling capability in the 3.0-to-5.0-μm window.

FACILITIES AND PROCEDURES USED IN ATMOSPHERIC-TRANSMISSION FIELD MEASUREMENTS

Extinction Measurements

The DF-laser-line extinction measurements augment the SMI data by providing actual transmission values for the calibration of the spectra at several DF laser lines. The particular lines used were chosen to provide as wide a dynamic range of transmissions as possible while spanning the 3.6-to-4.1-μm interval. Light from a low-power DF laser is transmitted over a 5.1-km path (A to B in-Fig. 1). It is sent from a 0.9-m-diameter Cassegrainian telescope to a 1.2-m-diameter Newtonian telescope (Fig. 3). The amount

of radiation is measured as it is sent and received, and, when account is taken of optical losses in the measurement system, the atmospheric transmission is a result.

Figure 4 shows the setup of the transmitter trailer at site A. Figure 5 shows the receiver trailer at site B.

The flat turning mirror seen in Figs 5c and 5d directs the reflected beam into the spectrometer room of the trailer (Fig. 2), where it is directed either into the SMI or GFCS instruments by additional folding mirrors. During the extinction measurements the bench shown in Fig. 5d holds the mobile detector (Fig. 3) near the secondary focus of mirror E1. The mobile detector (not photographed) is removed when either SMI or GFCS measurements are performed with a graybody instead of the laser source at the transmitter end of the experiment. The small HeNe alignment laser shown mounted in Fig. 5d is used to align the various optical elements in the receiver optical train to both the beam reflected from the 1.2-m collector mirror and to the SMI or GFCS instruments.

Scanning Michelson Interferometer System and Operating Procedures

An IDAC Model 1001 scanning Michelson interferometer (SMI) was used to obtain high-resolution atmospheric-transmission spectra in the 3.8-μm region. For these measurements a CaF_2 beamsplitter and an InSb detector were used. The instrument and its associated

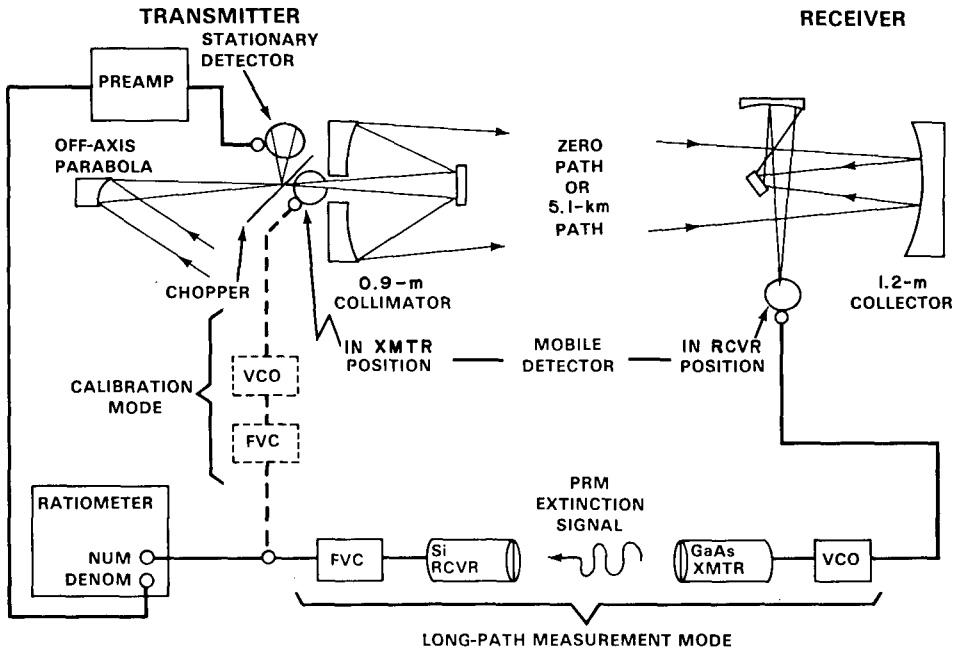

Fig. 3—System for measuring DF-laser line. Light from the DF laser is incident on the off-axis parabola at the upper left

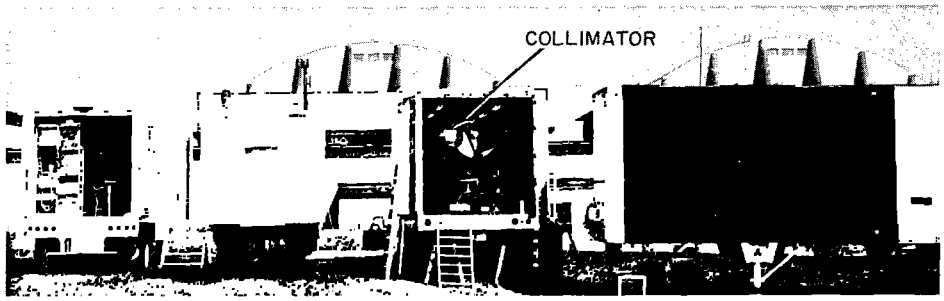

(a) Office trailer (with meteorological measuring equipment), pump trailer, transmitter trailer, and supply trailer

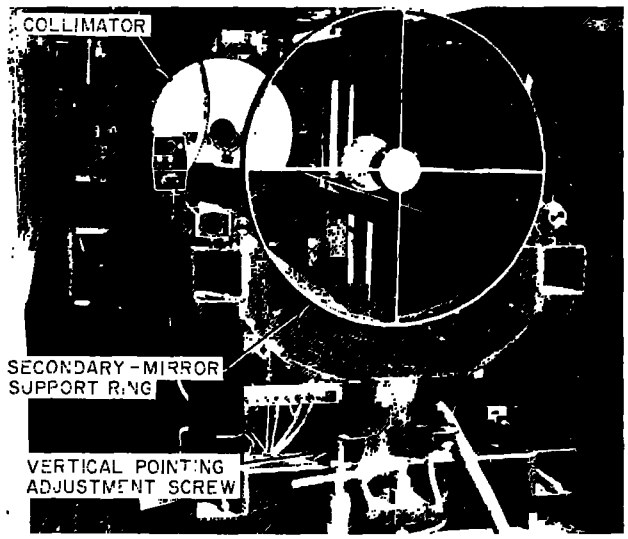

(b) Front view of the telescope frame

(c) Combustion-driven CW DF laser and laser cavity optics. The sine-drive mount is moved to the left of its normal position for visibility in the photograph.

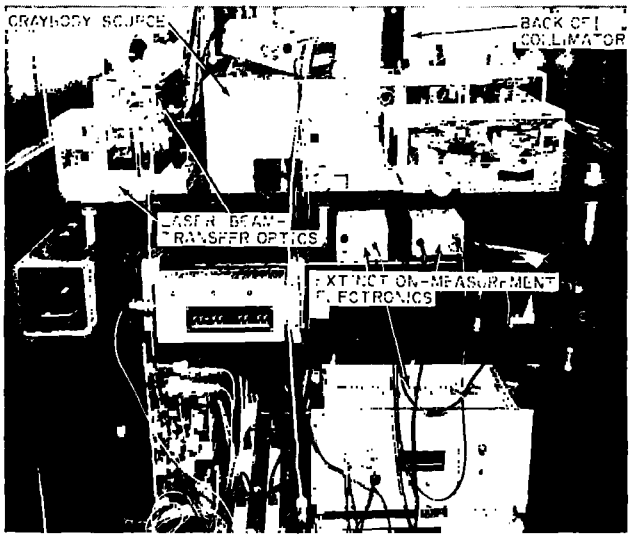

(d) Rear view of the telescope frame

Fig. 4—Transmitter and supporting equipment at site A. For orientation, the 0.9-m-diameter Cassegrainian telescope mirror (collimator) is labeled in each photograph.

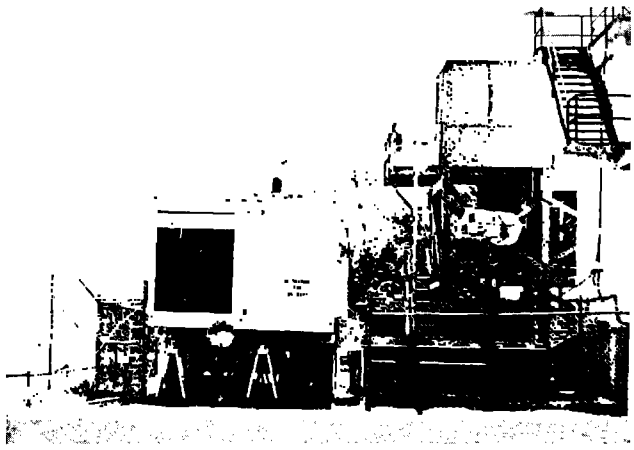

(a) Receiver trailer, with the rollup door open. The small searchlight is used in initial alignment of the transmitter telescope. The stands below the trailer frame support the optical bench carrying the demagnifying optics.

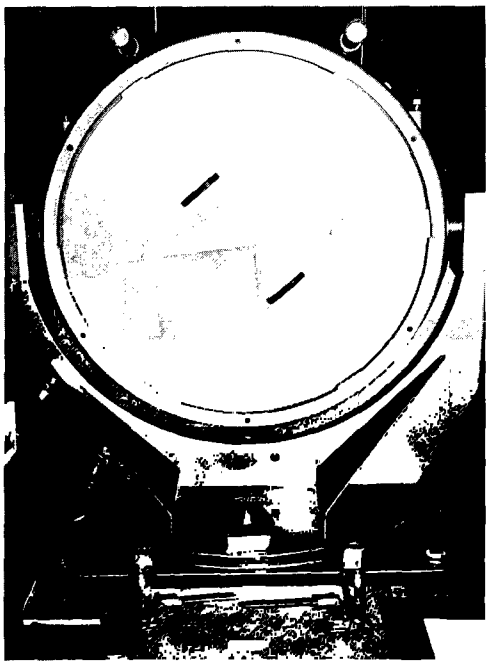

(b) The 1.2-m-diameter collector mirror (P1 in Fig. 2), with protective cover in place

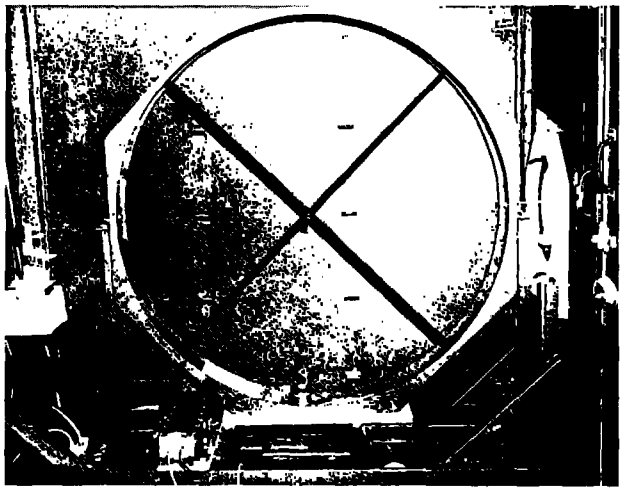

(c) View inside the closed rollup door showing the 1-cm-minor-diameter Newtonian mirror (F1 in Fig. 2) at the center, ellipsoidal mirror E1 at the right, and flat turning mirror F2 at the left. The GaAs data-link transmitter (Fig. 3) used to relay received signal information to the ratiometer in the transmitter trailer is at the lower left of the frame supporting F1.

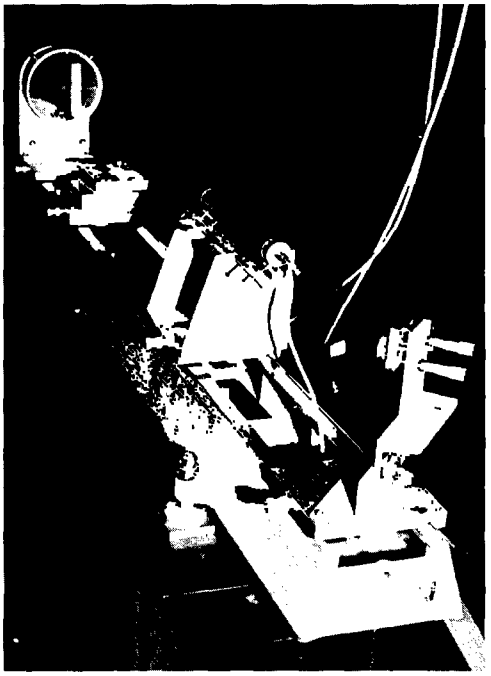

(d) Parabolic mirror (far end) used to recollimate the light from E1, flat turning mirror F2 (near end), and HeNe alignment laser

Fig. 5—Receiver at site B

data system are described in detail in Ref. 7. The locations of the SMI optical head and the SMI data console in the receiver trailer are shown in Fig. 2. Figure 6 shows the optical-table mounting used for the SMI head.

Figure 7 shows the SMI data console. At the left is the Kennedy incremental digital tape recorder used for storage of recorded interferograms or spectra. A Texas Instruments keyboard terminal used for entering the interferometer operating commands and for controlling data-processing procedures is immediately to the right of the tape recorder. To the right of the keyboard terminal is a CRT display monitor used for monitoring interferometer-scan reproducibility (synchronism of the white light and HeNe laser reference interferometer signals) and to observe sampled interferograms and spectra prior to plotting. The electrostatic high-speed digital plotting terminal used to produce permanent records of spectra is shown at the extreme right. The spectral plots contained later in this report were photographically copied directly from the plotter output.

For the initial phase of the operations at the Patuxent River NAS, an interferogram of 8-cm optical retardation was sampled at 2^{17} (128K) equally spaced points. To reduce noise in the resultant spectrum, 100 interferometer scans were combined prior to computing the Fourier transform. The entire process required approximately 20 minutes of sampling time and another 5 minutes of computer processing time.

Gas Filter Correlation Spectrometer

A gas filter correlation spectrometer (GFCS) has been constructed by SAI, Ann Arbor, Michigan, and was delivered to the NRL IMORL team on 15 September 1976 for field tests at the Patuxent River NAS. The GFCS measures integrated molecular HDO density in a path between transmitter and receiver sites. When the HDO/H_2O abundance ratio is known or is assumed ($\approx$0.03%), this measurement gives H_2O content in the path. Integral H_2O density along the transmission path provides an invaluable input to the DF

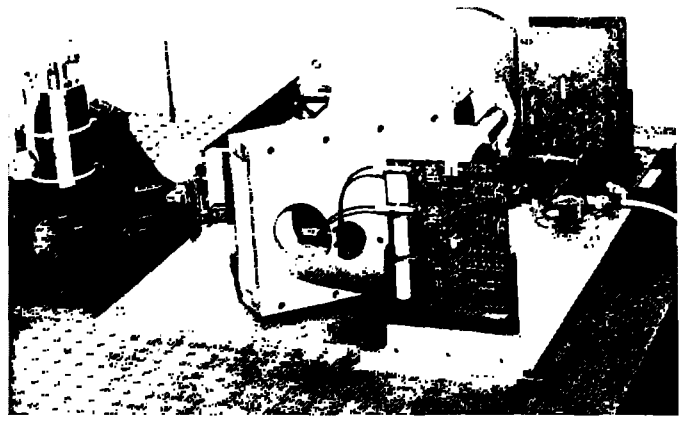

Fig. 6—SMI head on an optical table. The InSb detector is at the left; it is illuminated by a mirror cropped out of the photograph.

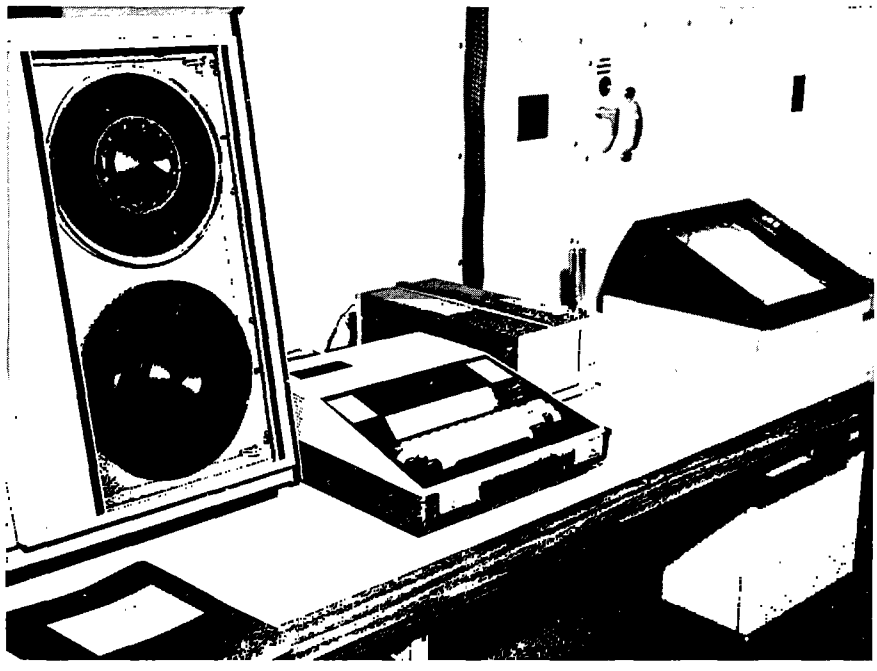

Fig. 7—SMI data console

extinction measurement in the field by quantifying strong molecular absorption.

A graybody source (obtained from the Perkin-Elmer Corporation and operating at 1385 K) is focused through a 750-Hz chopper and coupled into the IMORL transmitting telescope. As the beam traverses the atmospheric path, part of the radiation is selectively absorbed by the molecular HDO constituent, and the remaining energy passes into the receiver telescope. A portion of the beam that enters the GFCS (Fig. 8a) is then diverted directly through the bandpass filter (18) into the InSb detector (19) by a beamsplitter (7). The remaining portion of the beam after reflection from the concave mirror (5) is chopped at 45 Hz and alternately passed through a neutral-density filter (11) or through a White cell (14) containing a fixed amount of HDO. Each of these alternate beams is retroreflected through the bandpass filter (18) onto the detector (19). The neutral-density filter provides a nonstructured transmission which is balanced against the average of the structured transmission of the HDO in the White cell. The modulation thus induced on the detector output at 45 Hz, when normalized to the nonchopped signal, is then proportional to atmospheric HDO content through correlation with the HDO structure in the cell. By normalizing the modulation signal to the 750-Hz signal at the receiver, the modulation signal will be unaffected by shifts in source intensity and overall atmospheric transmission. External optical losses, detector response, and drift in electronics are common to both legs of the 45-Hz chopped signal and thus produce no change in the modulation signal. Figure 9 shows the GFCS as installed in the receiver van. A more detailed description of the GFCS and its calibration procedure is given in Ref. 7.

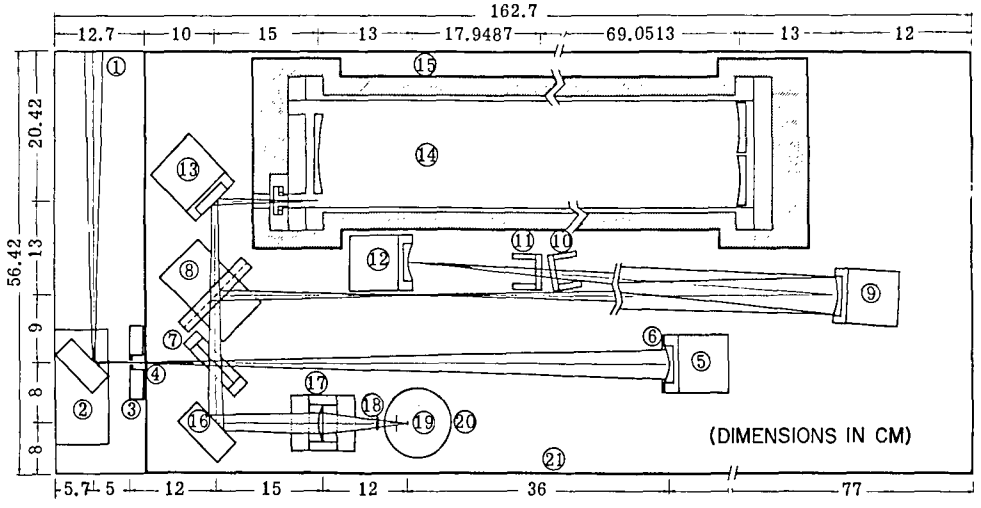

Fig. 8a—Gas filter correlation spectrometer: (1) entering beam, (2) flat mirror, (3) mount, (4) entrance aperture, (5) concave mirror, (6) field aperture, (7) beamsplitter, (8) 45-Hz chopper mirror, (9) concave mirror, (10) sapphire flat, (11) neutral-density filter, (12) concave mirror, (13) flat mirror, (14) White cell, (15) White-cell heater, (16) flat mirror, (17) As_2S_3 lens, (18) bandpass filter, (19) InSb detector, (20) detector dewar, and (21) mounting base plate.

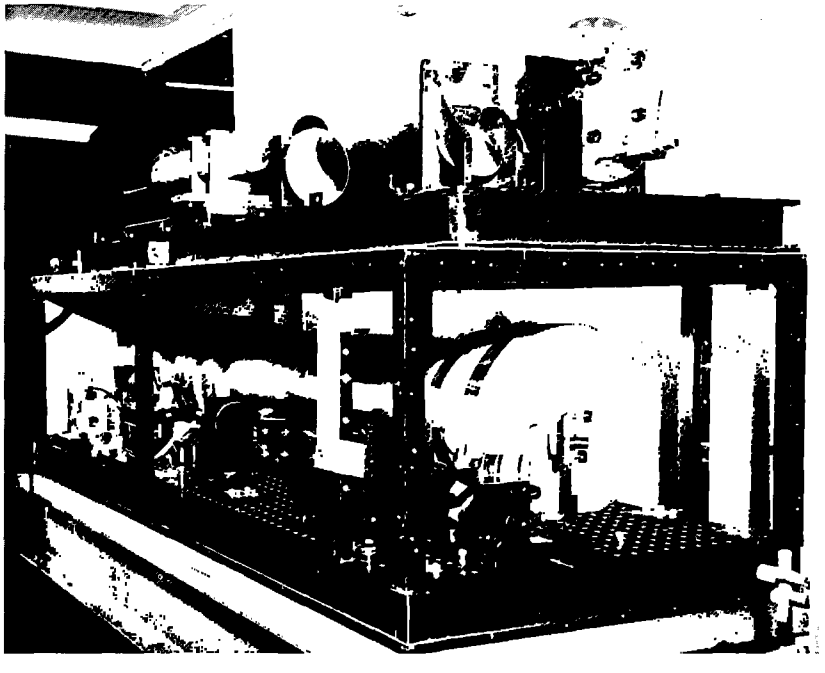

Fig. 8b—Gas filter correlation spectrometer as installed in the receiver van, with the dust cover removed. The GFCS is on the lower section, arranged not as diagramed in Fig. 8 but inverted left to right. The upper section holds a calibration cell with a known amount of HDO (to the right of small calibration cell for other gases), a graybody source (hidden), and a chopper and beam-directing optics (also hidden).

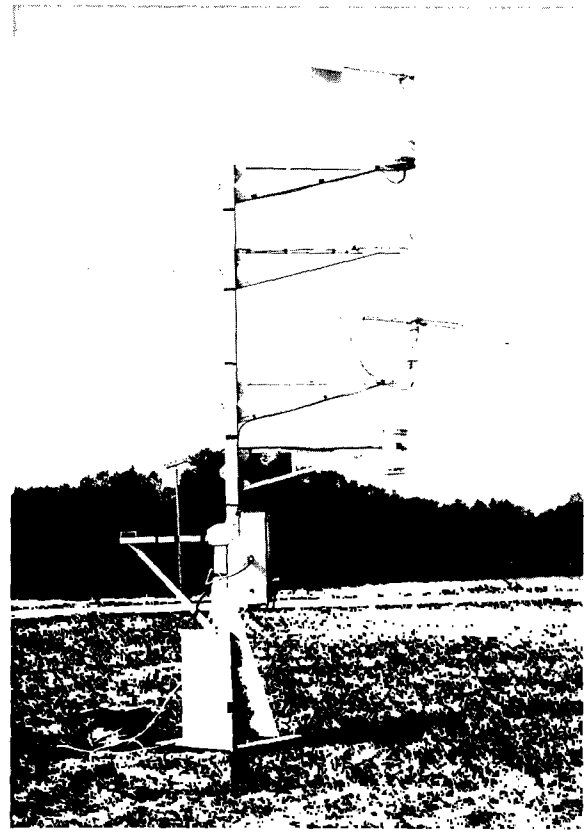

Fig. 9—Meteorological sensors near site A

Determination of Attenuation Coefficient at 0.65 μm

The attenuation coefficient at 0.65 μm was determined visually by means of a telephotometer [10,11]. This is an optical pyrometer which has been modified by the addition of a telephoto lens. The attenuation coefficient was determined by measuring the radiance of a suitable black target, in this case a 3.5-by-14-m opening in a large hangar, and also the radiance of the adjacent horizon sky. These radiances are then applied to the Koschmieder relationship, which relates luminance to attenuation. In its basic form the relationship is

$$\frac{B_H - B_T}{B_H} = T = e^{-\sigma X},$$

where B_H is the horizon radiance at 0.65 μm, B_T is the black-target radiance at 0.65 μm, σ is the attenuation coefficient at 0.65 μm, X is the distance between the observer and the black target (5.1 km), and T is the transmission over X at 0.65 μm. In this simplified form the target is black and the measurement is made in a spectral region of minimal absorption, so that the observed attenuation is caused by molecular and aerosol scattering. In practice the apparent spectral brightness temperature of the target and horizon sky is determined by the optical pyrometer at 0.65 μm. From the known blackbody spectral

radiance as a function of temperature, the attenuation coefficient is determined from the Koschmieder relationship. For example on 22 September 1976 at 1100 the observed target brightness temperature was 950°C and the horizon sky was 1055°C. The corresponding spectral radiances are 1.56 and 6.37 W cm^{-2} sr^{-1}, which result in a transmission value of 0.76 and a σ value of 0.055 (km^{-1}) at 0.65 μm.

Micrometeorological Measurement Instrumentation

Two micrometeorological stations are used in these field experiments for monitoring local weather conditions at each end of the propagation path. A description of the various sensors used in these systems is presented in Section C7 of Ref. 7. Figure 9 shows the various sensors arrayed on a supporting tower in the vicinity of the transmitter site now in use (site A, Fig. 1).

The signal-processing electronics and Monitor Laboratories data-acquisition system associated with the transmitter meteorological system have been relocated from an electronics trailer not currently in use in this series of experiments to the office trailer shown in Fig. 4a. The electronics racks were arranged (Fig. 10) to keep subsystems close together and to optimize the human-engineering aspects. Data tapes obtained during the phase of the experiment covered by this report will be processed once computer reduction

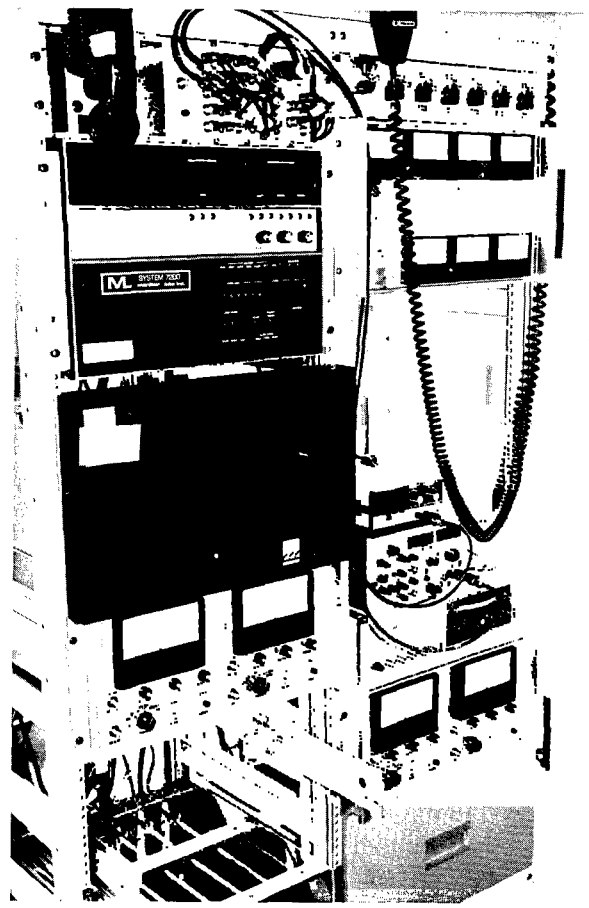

Fig. 10—Meteorological-sensor electronics racks as viewed from inside the office trailer at the transmitter (Fig. 4a)

programs which include reduction routines for extinction data (recorded on the same digital tape) are completed.

Representative determinations of air temperature, dew point, and relative humidity were made by periodic visual readings of the data-acquisition-system digital voltmeter (DVM), and these data are presented in the following section.

Meteorological data including aerosol distributions were recorded digitally at the receiver end of the path (site B) using a Particle Measurement Systems (PMS) data acquisition system incorporated into a mobile meteorological/aerosol monitoring van. A sensor array identical to that shown in Fig. 9 is deployed several meters from the van and used for sampling wind conditions, dew point, air temperature, and solar flux. A second tower next to the meteorological sensor array supports the PMS aerosol spectrometer probes. Information on the aerosol measurement system can be found in Ref. 7.

The data tapes containing meteorological and aerosol data taken at the receiver site are subsequently reduced at NRL using NRL's Texas Instruments ASC computer system. Using existing programs, 6-minute-average tabulations of the various meteorological parameters and aerosol distributions are obtained. Additionally a card deck containing the same information is punched and subsequently read using a batch card reader terminal connected to the CDC KRONOS time-sharing computer system. Once the data files are stored in the KRONOS library, detailed Mie scattering calculations and time-history plots for each meteorological parameter can be obtained using existing programs.

FIELD-MEASUREMENT RESULTS

Extinction Measurements

Two sets of DF laser extinction measurements were taken using the 5.1-km path at the Patuxent River NAS (Fig. 1). The results of these measurements are shown in Table 2. The first two columns list the DF-laser-line identification and the line position. The fourth and seventh columns list the measured transmission values, and the fifth and last columns list the extinction coefficient corresponding to the measured transmission values. The average transmission values listed in column seven (lower portion of table) for the run taken on day 268 were used to calibrate the SMI spectra in terms of absolute transmission over the spectral interval 2500 cm^{-1} to 2800 cm^{-1}.

High-Resolution Transmission Spectra

Spectra were taken using the 5.1-km path at the Patuxent River NAS on day 268 with the graybody source and transmitter/receiver optical systems described previously in this report (and in additional detail in Ref. 7). To accurately determine the spectral absorption at the DF laser frequencies for which extinction measurements were made, the infrared absorption spectrum was overlayed on a multiline DF laser emission spectrum. The (relative) spectral amplitudes at the DF laser line positions (locations of the laser lines on the SMI-generated spectrum plot) were measured and then combined with the absolute atmospheric transmissions using the laser measurements to determine a (wave number-dependent) normalization factor for this spectral region.

Table 2—DF Laser Extinction Measurements

DF Laser Line	Wave Number (cm^{-1})	Day 266 (22 September 1976)			Day 268 (24 September 1976)		
		Time	Transmission T	α (km^{-1})	Time	Transmission T	α (km^{-1})
$P_2 8$	2631.07	1609	0.818 ± 0.038	0.040 ± 0.009	1522	0.802 ± 0.034	0.044 ± 0.008
$P_2 7$	2655.86	1611	0.802 ± 0.037	0.044 ± 0.009	1524	0.606 ± 0.025	0.099 ± 0.008
$P_2 5$	2704.00	1614	0.855 ± 0.039	0.031 ± 0.009	1527	0.792 ± 0.033	0.046 ± 0.008
$P_1 8$	2717.54	1616	0.709 ± 0.033	0.068 ± 0.009	1528	0.580 ± 0.037	0.108 ± 0.012
$P_1 7$	2742.99	1618	0.859 ± 0.040	0.030 ± 0.009	1530	0.793 ± 0.036	0.046 ± 0.009
$P_1 6$	2767.97	1619	0.788 ± 0.036	0.047 ± 0.009	1532	0.660 ± 0.030	0.082 ± 0.009
$P_1 7$	2742.99	1621	0.865 ± 0.040	0.029 ± 0.009	1534	0.817 ± 0.038	0.040 ± 0.009
$P_1 8$	2717.54	1622	0.685 ± 0.032	0.075 ± 0.009	1537	0.554 ± 0.035	0.117 ± 0.012
$P_2 5$	2704.00	1623	0.843 ± 0.039	0.034 ± 0.009	1539	0.774 ± 0.033	0.051 ± 0.008
$P_2 7$	2655.86	1625	0.738 ± 0.034	0.060 ± 0.009	1541	0.633 ± 0.027	0.091 ± 0.008
$P_2 8$	2631.07	1627	0.834 ± 0.038	0.036 ± 0.009	1543	0.789 ± 0.033	0.047 ± 0.008
$P_3 5$	2617.39	1629	0.871 ± 0.040	0.027 ± 0.009	1544	0.846 ± 0.054	0.033 ± 0.012
$P_2 10$	2580.10	1631	0.681 ± 0.031	0.076 ± 0.009	1547	0.657 ± 0.030	0.083 ± 0.009
$P_2 12$	2527.39	1632	0.831 ± 0.038	0.037 ± 0.009	1548	0.774 ± 0.036	0.051 ± 0.009
$P_2 10$	2580.10	1634	0.693 ± 0.032	0.073 ± 0.009	1550	0.663 ± 0.030	0.081 ± 0.009
$P_3 5$	2617.39	1635	0.869 ± 0.040	0.028 ± 0.009	1552	0.925 ± 0.059	0.015 ± 0.012
$P_2 8$	2631.07	1636	0.870 ± 0.040	0.028 ± 0.009	1555	0.802 ± 0.034	0.044 ± 0.008
Averages for Each Day's Run							
$P_1 6$	2767.97	–	0.788 ± 0.036	–	–	0.660 ± 0.030	–
$P_1 7$	2742.99	–	0.862 ± 0.040	–	–	0.805 ± 0.037	–
$P_1 8$	2717.54	–	0.697 ± 0.032	–	–	0.568 ± 0.036	–
$P_2 5$	2704.00	–	0.849 ± 0.039	–	–	0.783 ± 0.033	–
$P_2 7$	2655.86	–	0.771 ± 0.035	–	–	0.620 ± 0.026	–
$P_2 8$	2631.07	–	0.840 ± 0.039	–	–	0.789 ± 0.033	–
$P_2 10$	2580.10	–	0.687 ± 0.032	–	–	0.660 ± 0.030	–
$P_2 12$	2527.39	–	0.831 ± 0.038	–	–	0.774 ± 0.036	–
$P_3 5$	2617.39	–	0.869 ± 0.040	–	–	0.886 ± 0.057	–

Figure 11 shows the normalized spectral transmission obtained for the entire DF spectral region for a path of 5.1 km and 12.0 torr partial pressure of water vapor. A synthetic spectrum calculated for a 5.1-km atmospheric path containing 12 torr of water vapor is shown in Fig. 11 for comparison to the normalized SMI spectra. The comparison shows excellent agreement between the measured and calculated spectra in terms of line structure and the relative line strengths. The major differences between the calculated and measured spectra stem from two factors. The observed spectrum includes transmission losses caused by aerosol scattering while the calculation does not and the calculation shows slightly lower transmission at the line centers of the strong absorption lines due to HDO.

Figure 12 is an SMI spectrum taken over the 5.1-km path with the multiline DF laser source. This spectrum was used in the transmission-spectrum normalization described above. Figure 13 is a high-dispersion plot showing a composite of the atmospheric transmission spectrum and the DF laser emission spectrum in the region from 2713 cm^{-1} to 2722 cm^{-1}. The comparison shows approximately 50% transmission at the center of the $P_1 8$ DF laser line at 2717.54 cm^{-1}.

Gas Filter Correlation Spectrometer (GFCS) Measurements

GFCS measurements commenced at the "zero-path" site with approximately 70 meters of path length between the transmitter and receiver vans on 17 September 1976. As shown in Table 3, modulation signals produced by multiple passes through the source White cell provided stable calibration signals from day to day. With the exception of 22 September the modulation signals did not deviate more than 5% from the curve shown in Fig. 14, which represents an average of the field calibration measurements. The lower modulation signal earlier in the day on 22 September seems to be the result of the operating the White cell at lower temperatures, beginning with 18.9°C, since the modulation signal strength climbed linearly and approached the curve shown in Fig. 14 as the air temperature rose during the day. This represents a significant dependence of calibration on source cell temperature ($\approx 1\%/°C$) and may reflect a problem with dependence on ambient air temperature along the path.

The agreement between GFCS-derived water-vapor-pressure values and the fixed-point (meteorological-station) measurements of dew point at the transmitter and receiver positions shown in Fig. 15 is preliminary. The large error bars on the first three days of operation reflect the fact that a path length of 70 m was used. On 22 September measurements were begun using the 5.1-km path, and agreement between the GFCS and the meteorological-station dew point measurements is good. Measurements on 23 and 24 September (Table 3) were restricted to source calibration due to the priorities of operating the SMI, which uses the same source as the GFCS.

Two problem areas which will be addressed in subsequent measurements are the temperature dependence of the GFCS calibration and the sensitivity of the instrument to orientation of the input beam as it passes through an alignment field stop. The temperature dependence of the GFCS calibration involves both the HDO-calibration-cell temperature and ambient-air temperature along the path, both of which are independent parameters in the present configuration.

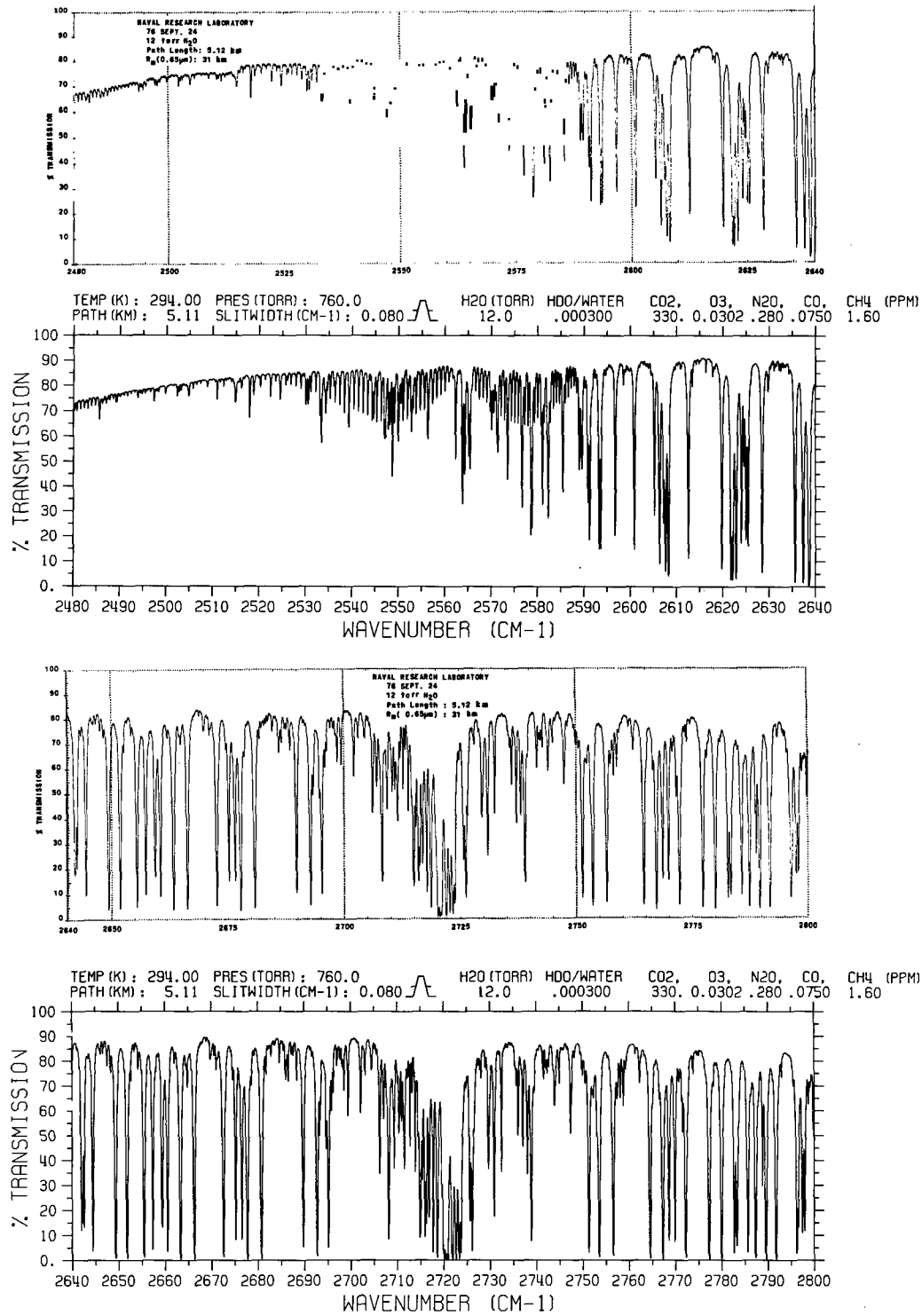

Fig. 11—Comparison of the normalized spectral transmission on day 268 (top strip, continued by the third strip) with a calculated spectrum (second and fourth strips)

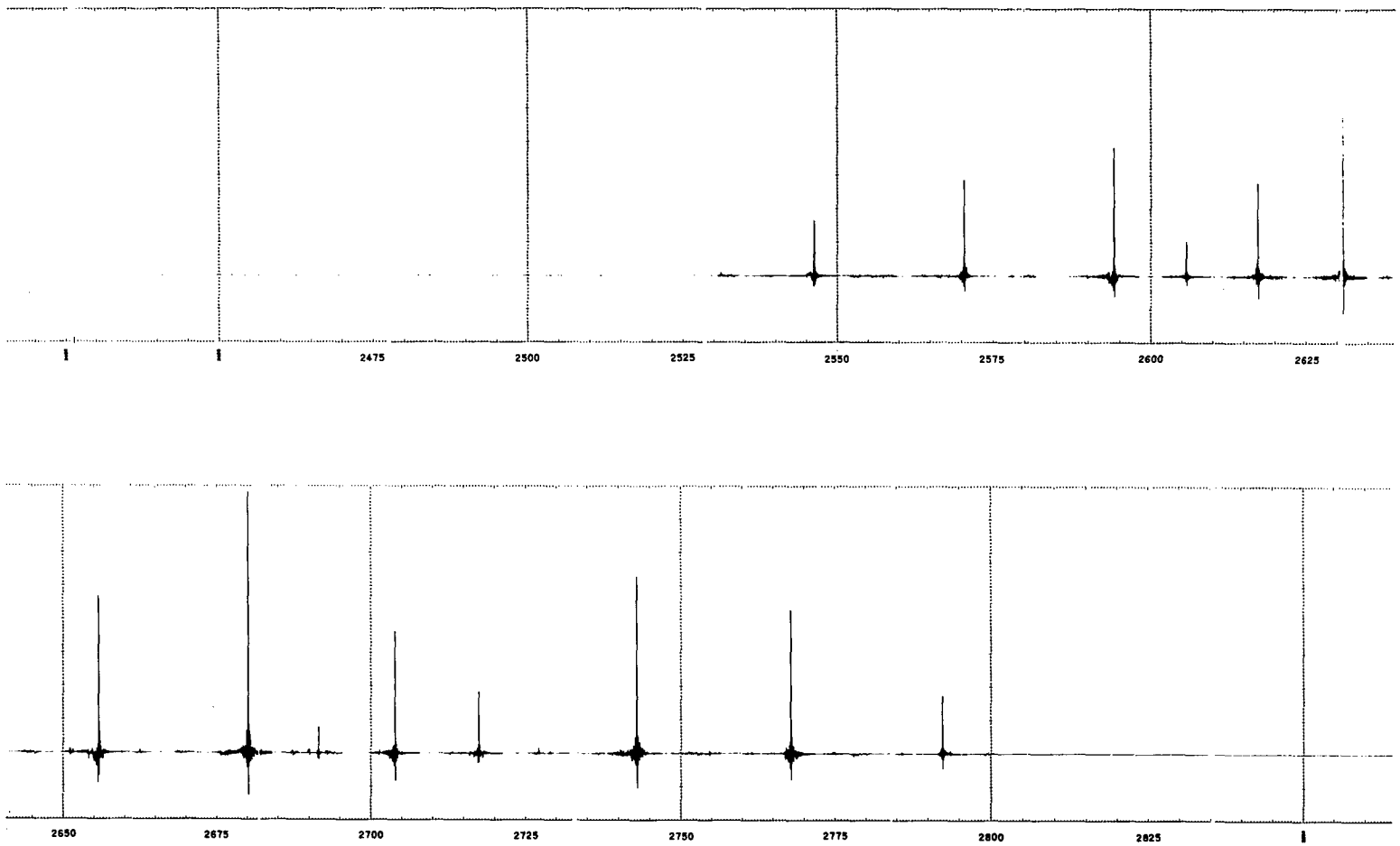

Fig. 12—Multiline DF-laser spectrum obtained with the SMI, used in precisely locating the DF laser lines to calibrate the measured plot in Fig. 11

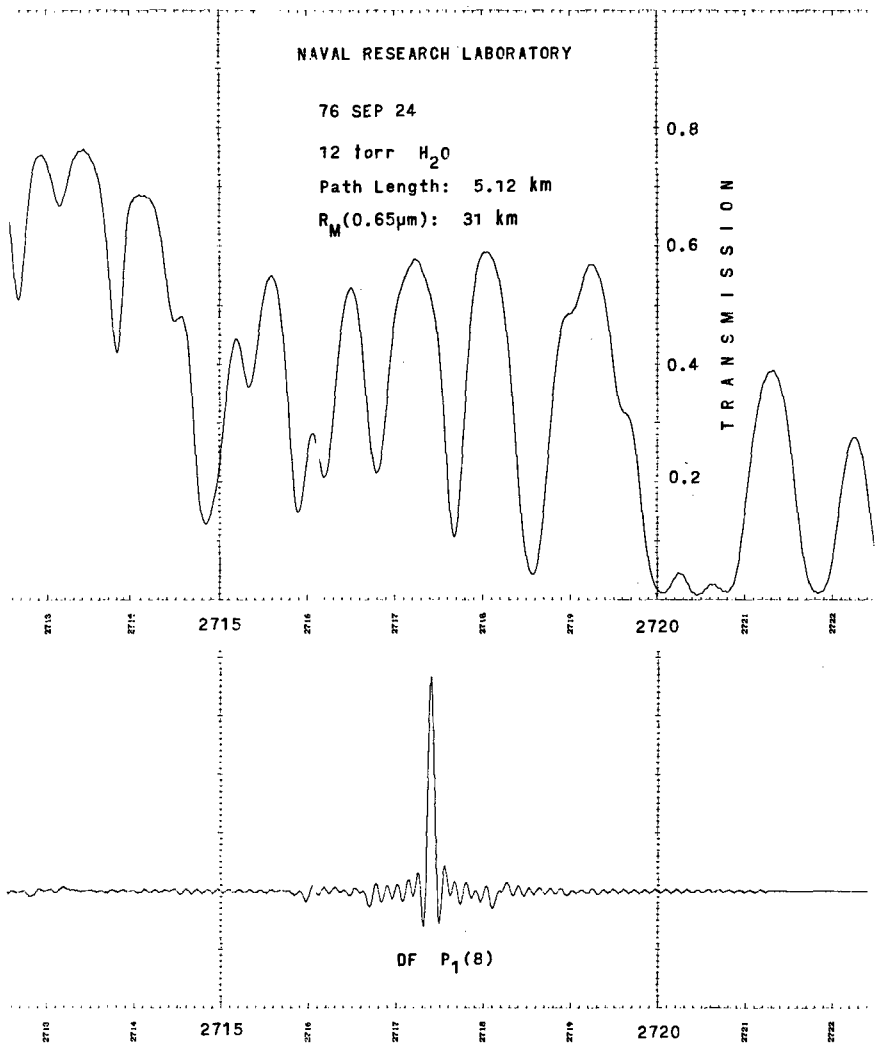

Fig. 13—Comparison of the transmission spectrum and the DF laser emission spectrum. Only a small portion of the spectral region is shown.

Table 3—GFCS Field Calibration Data

Date	Modulation (%)	No. of Passes Through the Calibrating White Cell	Time	Calibrating White Cell Temperature (°C)	Path Length (m)
9-17-76	7.52	20	1500	26.1	(*)
	7.51	20	1550	–	(*)
	6.65	16	–	–	(*)
	0.25	–	–	–	70
	5.61	12	–	–	(*)
	4.36	8	–	–	(*)
	2.70	4	–	–	(*)
9-18-76	2.68	4	1000	25.6	(*)
	0.23	–	–	–	70
	2.65	4	1115	–	(*)
	4.29	8	–	–	(*)
	5.59	12	–	–	(*)
	6.57	16	–	–	(*)
	7.47	20	–	–	(*)
	8.21	24	–	–	(*)
	8.89	28	1215	–	(*)
9-20-76	2.55	4	1100	25.6	(*)
	4.27	8	–	–	(*)
	5.64	12	–	–	(*)
	6.63	16	–	–	(*)
	7.48	20	–	–	(*)
	8.29	24	–	–	(*)
	8.95	28	1215	–	(*)
	9.59	32	–	–	(*)
	0.16	–	1230	–	70
9-22-76	3.78	–	1000	18.9	5115
	2.29	4	–	–	(*)
	3.95	8	–	–	(*)
	5.12	12	–	–	(*)
	6.28	16	1345	21.1	(*)
	5.22	12	–	–	(*)
	3.50	–	1500	–	5115
	4.27	8	1610	–	(*)
	3.55	–	1700	25.6	5115
9-23-76	4.30	8	–	25.6	(*)
9-24-76	4.30	8	–	–	(*)
	5.55	12	–	–	(*)

*White-cell path internal to GFCS used during calibration.

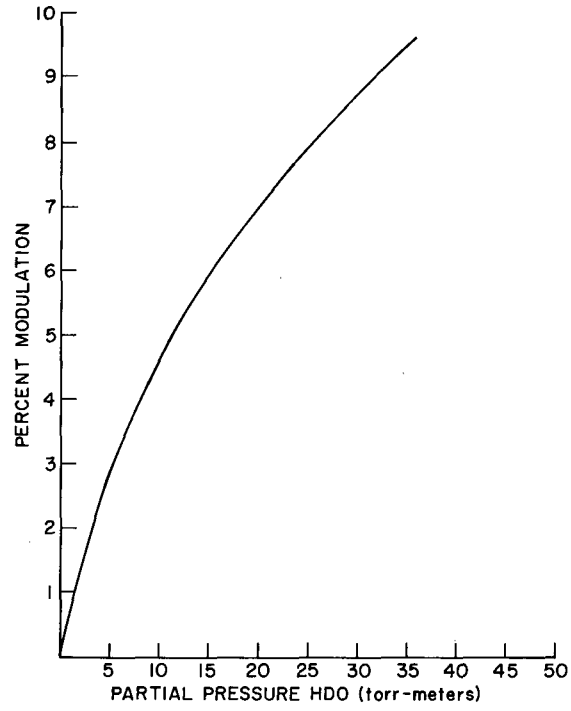

Fig. 14—Average of the GFCS calibration measurements using the HDO calibration cell

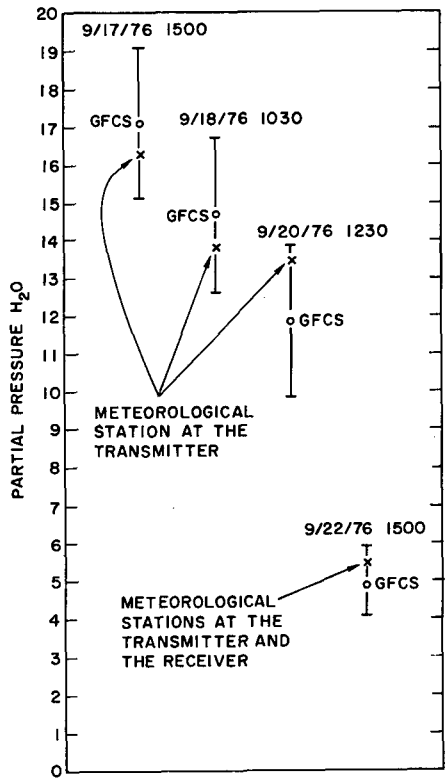

Fig. 15—Comparison of GFCS-derived values and fixed-point dew point measurements of water vapor pressures

Attenuation-Coefficient Measurements at 0.65 μm

Table 4 is a compilation of the visible attenuation-coefficient measurements performed at the indicated times. Column three of the table lists the transmission at 0.65 μm over a 5.5-km path between site B (Fig. 1) and aircraft hangers approximately 400 m north of site A. Column four is a tabulation of the corresponding attenuation coefficients at 0.65 μm.

Meteorological Measurements

Table 5 is a summary of visual readings taken at the indicated times using the meteorological station based in the office trailer and shown in Figs. 4a, 9, and 10. As previously described, data-reduction programs are currently being developed which will read the tapes containing both meteorological and extinction data parameters which are generated by the Monitor Laboratories 7200 data-acquisition system shown in Fig. 10.

Table 6 shows a sample of the output format of the data collected by the meteorological and aerosol monitoring system associated with the meteorological van at the receiver end of the 5.1-km path (site B, Fig. 1). Column-heading abbreviations are AT = air temperature (°C), DP = dew point (°C), WS = wind speed (m/s), WDH = wind direction horizontal (0 to 360° with 0° = north), BP = barometric pressure (millibars minus 1000), SR = solar radiation (cal cm^{-2} s^{-1}), abbreviations for various ac-line-voltage frequency and voltage monitors and spare channels, PPH2O = partial pressure of water vapor (torr), RH = relative humidity (%), and HR MN SC = measurement time in

Table 4—Results of Visible (0.65-μm) Attenuation-Coefficient Measurements

Date	Time	Transmission from Site B to 0.4 km North of Site A	Attenuation Coefficient σ (km^{-1})
9-22-76	1100	0.76	0.055
	1610	0.83	0.037
9-23-76	1130	0.73	0.063
	1500	0.73	0.063
	1650	0.82	0.040
9-24-76	0900	0.52	0.131
	1520	0.53	0.127
	1735	0.68	0.077
9-28-76	1000	0.55	0.120

Note: Rayleigh scattering at 0.65 μm is 0.0059 km^{-1}, which must be subtracted from the experimental values to give aerosol extinctions.

Table 5—Air Temperature, Dew Point, and Relative Humidity at the Transmitter Site

Date	Time	Air Temperature (°C)	Dew Point (°C)	Relative Humidity (%)
9-18-76	0957	21.46	15.62	71.0
	1023	22.56	16.16	67.0
	1242	25.56	15.14	52.6
	1502	26.04	13.82	46.9
	1543	26.40	15.20	50.2
	1550	25.12	14.80	52.7
9-20-76	1040	23.52	15.50	60.7
	1118	25.04	16.12	57.7
	1420	26.70	15.60	50.5
	1644	26.80	13.94	45.1
9-22-76	0952	16.12	5.48	49.4
	1140	18.30	5.26	42.3
	1334	19.64	3.04	33.2
	1701	19.88	3.28	33.3
9-24-76	1028	20.46	13.30	65.1

hours, minutes, and seconds. For each block of data these quantities are recorded on the first line, and the contents of the 45 aerosol counting bins (particles cm^{-3} bin^{-1}) spanning the range from 0.1 μm to 15 μm radius are printed in the remaining 45 entries.

Figure 16 is a sample of the aerosol distribution plots which are available using the CDC KRONOS time-sharing computer system and a Zeta plotter interfaced with the time-share terminal. Plots such as that shown in Fig. 15 are needed to verify correct operation of the aerosol monitoring equipment. The recorded distributions are then used in the Mie-scattering calculations to predict aerosol scattering and absorption at the wavelength of interest.

SUMMARY

This report summarizes the activities of the NRL atmospheric transmission measurement program for TQ 1976 (1 July through 30 September 1976). A summary of activities leading up to the fielding of an extensive atmospheric-transmission experiment is presented as well as progress on related supporting contract activities involving laboratory spectroscopic measurements and analysis. Initial data taken with a DF-laser-calibrated high-resolution atmospheric-transmission measurement system is presented along with concurrent meteorological measurements.

Table 6—Sample of Printout Containing Meteorological Measurements at Site B During DF-Laser-Extinction and SMI Spectral Measurements

THE YEAR IS 1976
THE DAY IS 268

AT	DP	WS	WDH	WDV	BP	SR	ACC	SPARE	ACV	SPARE	CHECK	PPH2O	RH	HR	MN	SC
19.5	13.4	4.23	137.	8.1	21.88	1.07	-1.1	0.00	-1.	0.00	3.10	11.54	68.1	14	36	0
2.50E 03	7.13E 02	1.46E 02	1.23E 01	4.31E 00	9.24E-01	3.08E-01	0.00E 00									
0.00E 00	0.00E 00	0.00E 00	0.00E 00	0.00E 00	0.00E 00	0.00E 00	0.00E 00									
1.23E 02	2.36E 01	5.43E 00	1.53E 00	2.96E-01	4.94E-02	1.48E-01	0.00E 00									
0.00E 00	0.00E 00	0.00E 00	0.00E 00	0.00E 00	0.00E 00	0.00E 00	0.00E 00									
7.72E-02	1.55E-01	5.46E-02	1.45E-02	5.56E-03	2.72E-03	1.30E-03	2.83E-04									
0.00E 00	0.00E 00	0.00E 00	0.00E 00	0.00E 00	0.00E 00	0.00E 00	0.00E 00									
19.6	13.8	4.32	85.	7.5	21.69	0.99	-1.1	0.00	-1.	0.00	3.10	11.79	69.0	14	42	0
2.52E 03	6.85E 02	1.48E 02	9.72E 00	4.03E 00	1.77E 00	7.86E-01	0.00E 00									
0.00E 00	0.00E 00	0.00E 00	0.00E 00	0.00E 00	0.00E 00	0.00E 00										
1.23E 02	2.15E 01	5.31E 00	1.02E 00	3.06E-01	0.00E 00	0.00E 00	0.00E 00									
0.00E 00	0.00E 00	0.00E 00	0.00E 00	0.00E 00	0.00E 00	0.00E 00										
7.42E-02	1.64E-01	5.74E-02	1.66E-02	6.69E-03	2.49E-03	1.47E-03	2.27E-04									
0.00E 00	0.00E 00	0.00E 00	0.00E 00	0.00E 00	0.00E 00	0.00E 00										
19.4	13.6	4.28	115.	7.1	21.68	0.93	-1.1	0.00	-1.	0.00	3.10	11.69	69.1	14	48	0
2.50E 03	6.83E 02	1.58E 02	1.03E 01	3.70E 00	1.33E 00	5.13E-01	0.00E 00									
0.00E 00	0.00E 00	0.00E 00	0.00E 00	0.00E 00	0.00E 00	0.00E 00										
1.16E 02	2.19E 01	6.07E 00	1.48E 00	2.96E-01	9.87E-02	1.48E-01	0.00E 00									
0.00E 00	0.00E 00	0.00E 00	0.00E 00	0.00E 00	0.00E 00	0.00E 00										
7.95E-02	1.52E-01	5.44E-02	1.30E-02	6.18E-03	3.00E-03	1.19E-03	2.27E-04									
0.00E 00	0.00E 00	0.00E 00	0.00E 00	0.00E 00	0.00E 00	0.00E 00										

AT	DP	WS	WDH	WDV	BP	SR	ACC	SPARE	ACV	SPARE	CHECK	PPH2O	RH	HR	MN	SC
19.6	13.5	4.22	47.	7.1	21.00	0.71	-1.1	0.00	-1.	0.00	3.10	11.58	67.9	15	18	0
2.22E 03	6.22E 02	1.27E 02	9.43E 00	2.65E 00	1.18E 00	5.89E-01	0.00E 00									
0.00E 00	0.00E 00	0.00E 00	0.00E 00	0.00E 00	0.00E 00	0.00E 00										
1.05E 02	1.68E 01	3.37E 00	7.15E-01	1.53E-01	1.02E-01	0.00E 00	0.00E 00									
0.00E 00	0.00E 00	0.00E 00	0.00E 00	0.00E 00	0.00E 00	0.00E 00										
7.60E-02	1.43E-01	5.05E-02	1.53E-02	4.37E-03	2.38E-03	9.64E-04	1.13E-04									
0.00E 00	0.00E 00	0.00E 00	0.00E 00	0.00E 00	0.00E 00	0.00E 00										
19.7	13.8	4.55	36.	6.7	20.86	0.76	-1.1	0.00	-1.	0.00	3.10	11.80	68.6	15	24	0
2.27E 03	6.77E 02	1.47E 02	9.55E 00	4.00E 00	2.16E 00	8.21E-01	0.00E 00									
0.00E 00	0.00E 00	0.00E 00	0.00E 00	0.00E 00	0.00E 00	0.00E 00										
1.11E 02	2.43E 01	4.25E 00	1.14E 00	3.95E-01	1.97E-01	1.48E-01	0.00E 00									
0.00E 00	0.00E 00	0.00E 00	0.00E 00	0.00E 00	0.00E 00	0.00E 00										
7.54E-02	1.54E-01	5.47E-02	1.47E-02	5.84E-03	2.72E-03	1.08E-03	2.27E-04									
0.00E 00	0.00E 00	0.00E 00	0.00E 00	0.00E 00	0.00E 00	0.00E 00										
19.6	13.7	5.11	7.	6.5	20.73	0.80	-1.1	0.00	-1.	0.00	3.10	11.77	68.9	15	30	0
2.33E 03	6.90E 02	1.53E 02	7.07E 00	3.93E 00	1.77E 00	9.82E-01	0.00E 00									
0.00E 00	0.00E 00	0.00E 00	0.00E 00	0.00E 00	0.00E 00	0.00E 00										
1.13E 02	2.21E 01	5.67E 00	1.07E 00	1.53E-01	5.10E-02	1.02E-01	0.00E 00									
0.00E 00	0.00E 00	0.00E 00	0.00E 00	0.00E 00	0.00E 00	0.00E 00										
7.64E-02	1.51E-01	5.20E-02	1.39E-02	4.54E-03	2.15E-03	9.64E-04	1.13E-04									
5.67E-05	0.00E 00	0.00E 00	0.00E 00	0.00E 00	0.00E 00	0.00E 00										
19.5	13.8	5.26	19.	6.5	20.68	0.78	-1.1	0.00	-1.	0.00	3.09	11.77	69.4	15	36	0
2.25E 03	6.82E 02	1.28E 02	8.52E 00	3.88E 00	1.13E 00	3.88E-01	0.00E 00									
0.00E 00	0.00E 00	0.00E 00	0.00E 00	0.00E 00	0.00E 00	0.00E 00										
1.09E 02	1.94E 01	4.10E 00	9.38E-01	1.48E-01	0.00E 00	1.48E-01	0.00E 00									
0.00E 00	0.00E 00	0.00E 00	0.00E 00	0.00E 00	0.00E 00	0.00E 00										
7.70E-02	1.56E-01	5.19E-02	1.45E-02	5.90E-03	2.10E-03	6.24E-04	1.13E-04									
0.00E 00	0.00E 00	0.00E 00	0.00E 00	0.00E 00	0.00E 00	0.00E 00										
19.5	13.7	4.83	27.	6.4	20.68	0.75	-1.1	0.00	-1.	0.00	3.09	11.69	69.0	15	42	0
2.11E 03	5.58E 02	1.16E 02	8.84E 00	4.12E 00	1.08E 00	1.08E 00	0.00E 00									
9.82E-02	9.82E-02	1.96E-01	0.00E 00	0.00E 00	9.82E-02	0.00E 00										
1.05E 02	1.66E 01	4.64E 00	6.63E-01	2.55E-01	0.00E 00	0.00E 00	0.00E 00									
0.00E 00	0.00E 00	0.00E 00	0.00E 00	0.00E 00	0.00E 00	0.00E 00										
7.21E-02	1.54E-01	5.38E-02	1.37E-02	6.41E-03	3.12E-03	1.30E-03	5.67E-05									
0.00E 00	0.00E 00	0.00E 00	0.00E 00	0.00E 00	0.00E 00	0.00E 00										
19.5	14.1	4.86	18.	6.1	20.46	0.73	-1.1	0.00	-1.	0.00	3.09	12.07	70.9	15	48	0
2.04E 03	5.67E 02	1.18E 02	8.52E 00	2.98E 00	1.33E 00	6.16E-01	0.00E 00									
0.00E 00	0.00E 00	0.00E 00	0.00E 00	0.00E 00	0.00E 00	0.00E 00										
1.01E 02	1.65E 01	4.74E 00	7.90E-01	9.87E-02	0.00E 00	0.00E 00	0.00E 00									
0.00E 00	0.00E 00	0.00E 00	0.00E 00	0.00E 00	0.00E 00	0.00E 00										
7.20E-02	1.54E-01	5.24E-02	1.53E-02	6.24E-03	2.95E-03	9.64E-04	2.27E-04									
0.00E 00	0.00E 00	0.00E 00	0.00E 00	0.00E 00	0.00E 00	0.00E 00										
19.4	13.7	4.68	21.	6.7	20.45	0.71	-1.1	0.00	-1.	0.00	3.09	11.74	69.5	15	54	0
1.96E 03	5.30E 02	1.15E 02	7.17E 00	2.65E 00	1.08E 00	4.91E-01	0.00E 00									
0.00E 00	0.00E 00	0.00E 00	0.00E 00	0.00E 00	0.00E 00	0.00E 00										
9.22E 01	1.54E 01	4.59E 00	1.12E 00	4.08E-01	2.04E-01	1.02E-01	0.00E 00									
0.00E 00	0.00E 00	0.00E 00	0.00E 00	0.00E 00	0.00E 00	0.00E 00										
7.14E-02	1.40E-01	5.13E-02	1.49E-02	6.01E-03	3.40E-03	1.64E-03	2.83E-04									
0.00E 00	0.00E 00	0.00E 00	0.00E 00	0.00E 00	0.00E 00	0.00E 00										

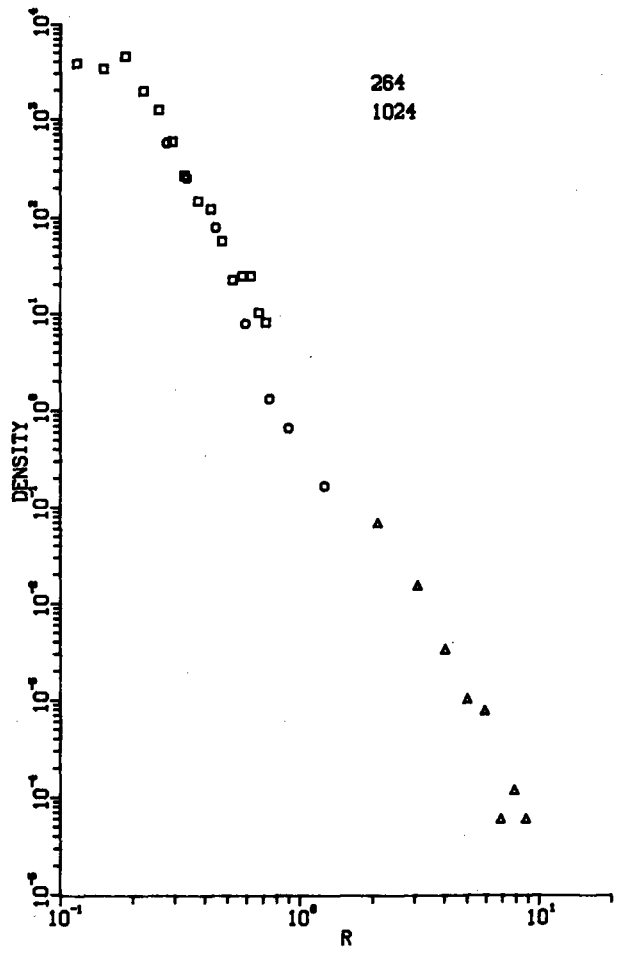

Fig. 16—Sample of the computer plots of aerosol distribution

ACKNOWLEDGMENTS

The authors acknowledge the continued encouragement and the programmatical and administrative support provided by Dr. D. Finkleman, Naval Sea Systems Command, PM-22/PMS-405, and Dr. P. B. Ulrich, Naval Research Laboratory, throughout the course of this work. Excellent shop support was provided in the preparation of the receiver optical system by NRL-CBD machine-shop personnel including M. Dement, J. Cox, and S. King.

Science Applications, Inc., Ann Arbor, Michigan, has played a key role in the work described herein. Specifically, design and construction of the GFCS device by D. R. Woods and R. E. Meredith is gratefully acknowledged. Additionally, generation of calculated atmospheric transmission spectra by D. R. Woods, R. E. Meredith, F. G. Smith, and J. P. Walker is greatly appreciated as being of fundamental importance in the use of the NRL atmospheric measurements.

REFERENCES

1. J.A. Dowling and P.M. Livingston, "Atmospheric Extinction Measurements for Several DF Laser Lines Near 3.8 μm," paper VI, International Laser Radar Conference, Sendai, Japan, 3-6 Sept. 1974.

2. J.A. Dowling et al., "Atmospheric Laser Propagation Measurements for 0.63-, 1.06-, 3.8-, and 10.6-μm Wavelengths," NRL Report, in preparation.

3. J.A. Dowling, K.M. Haught, R.F. Horton, G.L. Trusty, J.A. Curcio, T.H. Cosden, S.T. Hanley, C.O. Gott, and W.L. Agambar "Atmospheric Extinction Measurements at Nd-YAG and DF Laser Wavelengths Performed in Conjunction with JAN Propagation Tests, June-September 1975," NRL Report 8058, August 1977.

4. D.R. Woods, T.W. Tuer, and R.E. Meredith, "DF Laser Propagation Analysis, 1st Informal Report," SAI-76-002-AA, Apr. 1976.

5. D.R. Woods, T.W. Tuer, J.P. Walker, and R.E. Meredith "DF Laser Propagation Analysis, 2nd Informal Report," SAI-76-006-AA, Aug. 1976.

6. J.A. Dowling, "Atmospheric Transmission Measurements Using Infrared Lasers and Fourier Spectroscopy—Techniques, Results, and Comparisons to Computer Models," presented at the 20th Annual SPIE Conference, 23-27 Aug. 1976, San Diego, California (to appear in conference proceedings).

7. J.A. Dowling, R.F. Horton, G.L. Trusty, T.H. Cosden, K.M. Haught, J.A. Curcio, C.O. Gott, S.T. Hanley, P.B. Ulrich, and W.L. Agambar, "Atmospheric Transmission Measurement Program and Field Test Plan," NRL Report 8059, August 1977.

8. M.M. Shapiro and H.P. Gush, *Canad. J. Physics* 44, 949 (1966).

9. K.O. White, W.R. Watkins, and C.W. Bruce, "Water Vapor Line and Continuum Absorption Measurements in the Infrared," presented at the ODDR&E Optical/ Submillimeter Atmospheric Propagation Workshop, Colorado Spring, Colo., 6-10 Dec. 1976.

10. J.A. Curcio and K.A. Durbin, "Atmospheric Transmission in the Visible Region," NRL Report 5368, Oct. 1959.

11. J.A. Curcio and G.L. Knestrick, "Atmospheric Transmission Measurements with an Optical Pyrometer" (abstract), *J. Opt. Soc. Am.* 47, 113 (1957).